STUDY OF VORTEX RING DYNAMICS USING UVP

Yuichi Murai*, Hidekazu Kitaura*, Zhiying Xiao**, Peter J. Thomas**, Yasushi Takeda*

*Division of Mechanical Science, School of Engineering, Hokkaido University
N13W8, Sapporo, 060-8628, Japan, E-mail: murai@eng.hokudai.ac.jp
**Fluid Dynamics Research Centre, School of Engineering, University of Warwick
Coventry, AV4 7AL, UK, E-mail: pjt1@eng.warwick.ac.uk

ABSTRACT

The dynamics of a vortex ring generated at the tip of a nozzle which is fixed on the top of a cylindrical water tank are investigated using UVP (Ultrasound Velocity Profiler). The instantaneous velocity profiles on three ultrasound beams are obtained to reconstruct two-dimensional structure of vortex ring. The nozzle diameter is D_o=50mm and experiments were performed for varying piston speeds and strokes of the vortex ring generator. The measurement section is $5D_o$ from the vortex ring generator, at which the vortex ring involves the influence of transient structure before reaching developed state. The translational velocity, the diameter, and the length of the vortex ring are quantitatively evaluated from the two-dimensional velocity field as function of dimensionless piston stroke and Reynolds number. The results have shown that the vortex ring has a certain condition to be generated clearly in the initial developing region. The typical length scales coincide with earlier studies, and thereby the availability of UVP for the intermittent flow measurement has been confirmed.

Keywords: Vortex ring, UVP, Flow field reconstruction, Multi-dimensional flow measurement

INTRODUCTION

A vortex ring can be seen in various natural phenomena regarding intermittent fluid flow such as volcanic fumes and smoker's rings. It has a long history of research from various points of views from pure scientific study to advanced engineering application. Especially the vortex ring has been chosen as a good research target to obtain fundamental knowledge on flow transition or instability caused by nonlinear phenomena of fluid flow [1][2]. Recent topics associated with vortex rings are the mechanism of downburst as a motion of large vortex ring [3], the interaction of flame with vortex ring [4][5], the vortex ring generated by a bursting bubble [6], the sound noise generation by vortex-pairing [7], and the atomization of droplets in fuel injection for IC engines [8]. On the other hand, vortex rings have often been employed as paradigms to test flow measurement techniques such as LDV and PIV because the vortex ring is one of elementary structures of fluid flow expressed mathematically [9]. In the past characteristics of vortex rings, such as their translational velocity, the ring diameter, and the ring's axial length, was studied by means of dye visualization and LDV [10]. Recently velocity measurements based on digital image processing such as PIV was employed to investigate vortex rings [11][12].

In this study, UVP (Ultrasound Velocity Profiler,[13]) is used to acquire those parameters directly from the two-dimensional flow field, which is measured by three ultrasound transducers. Utilization of UVP allows us to measure the on-beam velocity profile at real time, thereby the suitable experimental condition for generating ideal vortex ring can be found in a short working time. In addition, the repetition of measurement for treating irregularity of the vortex is easily performed. In this paper we report first results on the flow measurement technique based on multiple channel UVP, the flow field reconstruction method, and the difference of internal structure accompanied with changing the piston speed and the piston stroke of a vortex ring generator.

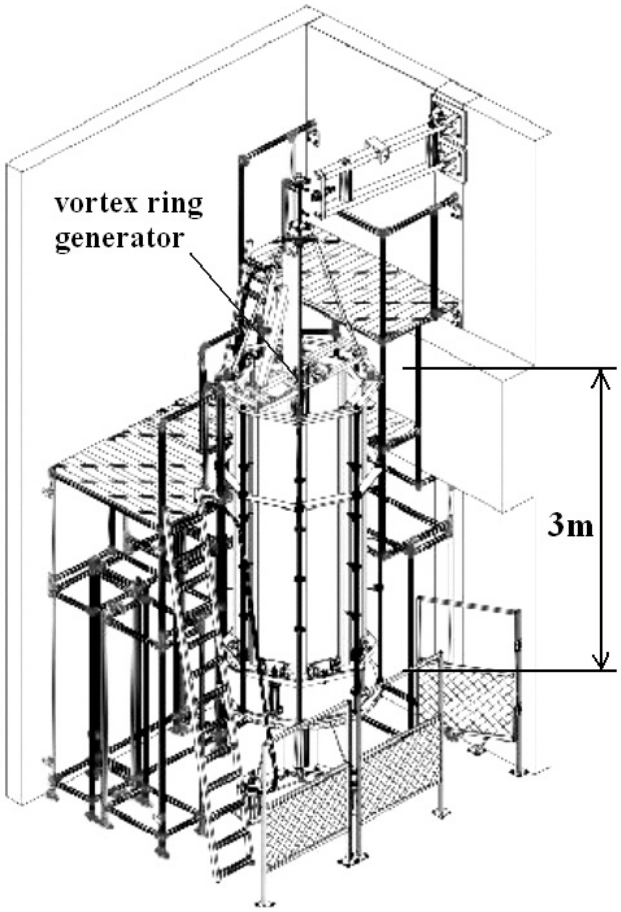

Fig.1 Overview of experimental facility

EXPERIMENTAL METHOD

Experimental facility

Fig.1 shows overview of experimental facility. A vortex ring generator, which is composed of a cylindrical nozzle and a reciprocating piston, is fixed on the top of a water tank with 3m heights and 1m widths. The vortex ring is emitted downward in water. The diameter of the nozzle D_0 is 50mm and the piston to push out the vortex ring is connected with a stepping motor controlled by computer, so the stroke S and the piston speed V are control parameters. The acceleration and the deceleration of the piston are fixed at 30m/s^2. The water temperature was 9.2 deg C, therefore, the kinematic viscosity is 1.30 x 10^{-6} m^2/s and the density is 0.998 x 10^3 kg/m^3. Vortex rings for 43 different parameter combinations were investigated – these test cases are summarized in Table 1. The numbers in the cells of Table 1 identify the number of the experiments.

Table 1. Experimental conditions

Piston Stroke D (mm)	Piston Velocity V (mm/s)						
	100	200	300	400	500	600	700
30	1	2	3	4	5	6	7
50	8	9	10	11	12	13	14
70	15	16	17	18	19	20	21
90	22	23	24	25	26	27	28
110	29	30	31	32	33	34	35
130	36	37	38	39			
150	40	41	42	43			

Injection of tracers

Hydrogen bubbles are used as fluid tracers for providing echo, i.e., ultrasound reflector. The bubbles are generated using two platinum wires of 0.5mm in diameter and 100mm in length. The wires are connected to a DC power by parallel circuit. 30V-DC power was enough to supply hydrogen bubbles with a sufficient number density around the target volume of the measurement. The mean bubble rise velocity was 20mm/s in quiescent water, so the mean diameter is estimated to be 0.27mm by assuming Levichi's drag coefficient (C_D=48/Re), which is around 1/5 of the wavelength of 4MHz ultrasound in water.

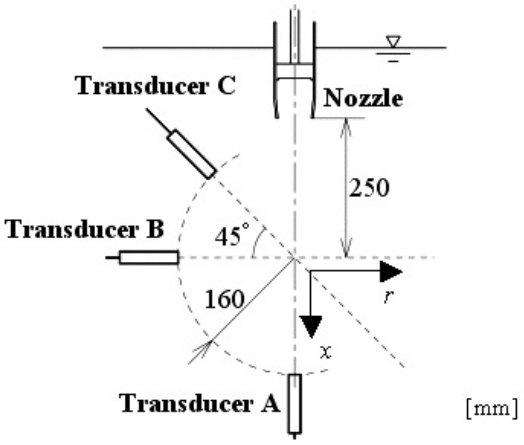

Fig.2 Definition of measurement space

Arrangement of ultrasound transducers

In order to obtain the velocity profiles on multiple measurement lines, three ultrasound transducers were mounted inside the tank as shown in Fig.2. The transducer A provides the axial (vertical) velocity component, the transducer B the lateral (horizontal), and the transducer C the oblique velocity component, respectively. The three ultrasound beams cross at x=250mm, i.e. 5 times the diameter of the vortex ring generator. The measurable radius from the cross point R is 160mm.

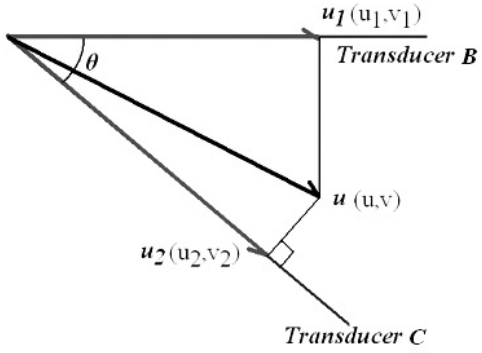

Fig.3 Velocity vector obtained by two velocity profiles

Reconstruction of two-dimensional flow

The vortex ring often has a three-dimensional structure in the initial region of the nozzle and in the transition region to turbulent flow before breaking up. However the primary flow is axisymmetic two-dimensional, and it is maintained in a certain distance from the nozzle. We have tried to measure the two-dimensional velocity vector field at the measurement space by combining multiple measurement data obtained in different direction. The velocity vector of the flow is calculated from two componential velocities, obtained by transducers B and C. As shown in Fig.3, the transducer B provides the lateral velocity $\mathbf{u}_1$ (u_1, v_1). Here u_1 is the lateral component, and v_1 the axial component. We set the transducer B in a horizontal plane so that v_1=0. The transducer C provides oblique components $\mathbf{u}_2$ (u_2,v_2) at the angle of θ=45 degree. Expressing the real velocity vector of the flow by $\mathbf{u}$ (u, v), the differential velocity vector ($\mathbf{u}_2$-$\mathbf{u}$) and $\mathbf{u}_2$ cross in perpendicular, therefore,

$$(\mathbf{u}_2 - \mathbf{u})\bullet\mathbf{u}_2 = 0 \tag{1}$$

The velocity component u of $\mathbf{u}$ corresponds to u_1 or the direct measurement velocity U_B since the transducer B is set in a horizontal plane, i.e.,

$$u = u_1 = U_B . \tag{2}$$

Hence, eq.(1) can be rewritten with the components by,

$$(u_1 - u_2)u_2 + (v - v_2)v_2 = 0. \tag{3}$$

This equation gives the velocity component v by the following form,

$$v = v_2 - \frac{u_2}{v_2}(u_1 - u_2) . \tag{4}$$

The velocity components of $\mathbf{u}_2$ (u_2, v_2) are calculated from the velocity U_c measured by the transducer C as follows,

$$u_2 = U_C \cos\theta , \tag{5}$$

$$v_2 = U_C \sin\theta . \tag{6}$$

Thus, the velocity components u and v are calculated by,

$$u = U_B \tag{7}$$

$$v = U_C \sin\theta - (\tan\theta)^{-1}(U_B - U_C \cos\theta) \tag{8}$$

The velocity vector field of the vortex ring can be reconstructed by assuming that the vortex ring keeps its two-dimensional flow structure in a short period or in a short distance. Namely, the vortex ring to be measured must not change its own structure in the measurement space within R=160mm. Fortunately, ordinary vortex rings are stable for a

certain long distance up to hundreds times as its diameter. Using this assumption or the phenomenological fact, the velocity vector field is calculated even though the local measurement timing differs dependent on the alignment of the transducers.

RESULTS AND DISCUSSION

Translational velocity

The translational velocity of vortex ring is obtained from the temporal change of the vertical velocity profiles measured by the transducer A. Fig.4 (a) shows samples of instantaneous profiles of the axial velocity. The core part of the vortex ring has downward velocity as shown in the graph, and this profile migrates with a translational velocity. After the peak velocity location in each profile is obtained as function of time as shown in Fig.3 (b), the translational velocity and the deceleration are measured by fitting the data with second order function. The typical deceleration of vortex ring was 10^{-3} m/s^2 which provided around 3% reduction of the translational velocity in the measurement space within R=160mm. The decelerations measured in some cases (Cases 3, 7,and 33) were more than 30% in the measurement space due to very unstable ring structure, however the translational velocity was defined as the mean value within the measurement space.

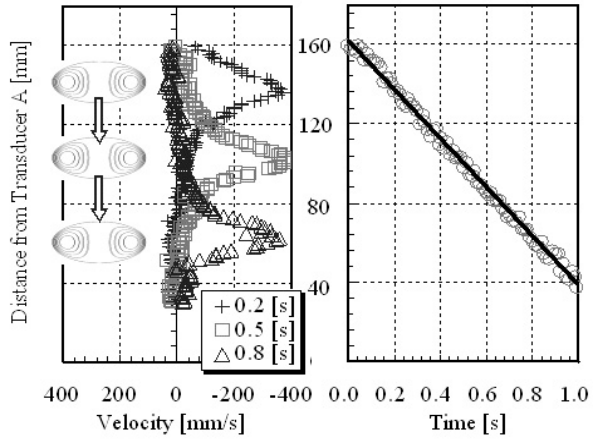

(a) velocity profiles (b) peak velocity location

Fig.4 Velocity profile measured by transducer A

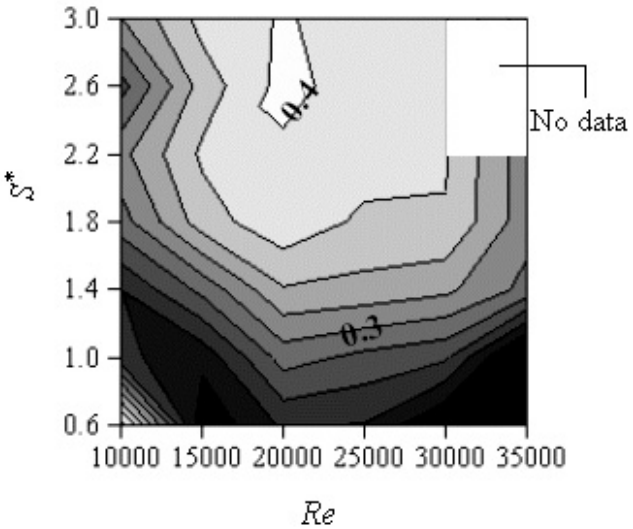

Fig.5 Map of dimensionless translational velocity

Fig.5 shows the measurement data of the translational velocity U^* which is non-dimensionalized by the piston speed V. A Reynolds number for the vortex ring is defined by Re=$V D_0/\nu$. The dimensionless piston stroke is defined by S*=S / D_0. The grayscale map expresses larger U^* as white while smaller as the black. According to the measurement results, U^* increases almost linearly with S^* and also with Re at $Re < 2.0 \times 10^4$ while U^* becomes almost constant at $Re > 2.0 \times 10^4$. This implies that, 1) vortex ring is undeveloped at $Re < 2.0 \times 10^4$, and is developed enough at $Re > 2.0 \times 10^4$ in the measurement space, 2) the translational velocity relative to piston speed reaches around 0.5 only in certain optimum condition while it has smaller value in case of small S^*.

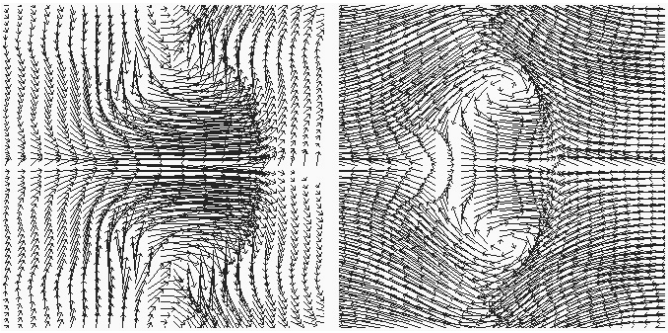

(a) absolute velocity (b) relative velocity

Fig.6 Velocity vector field of vortex ring for Case 24

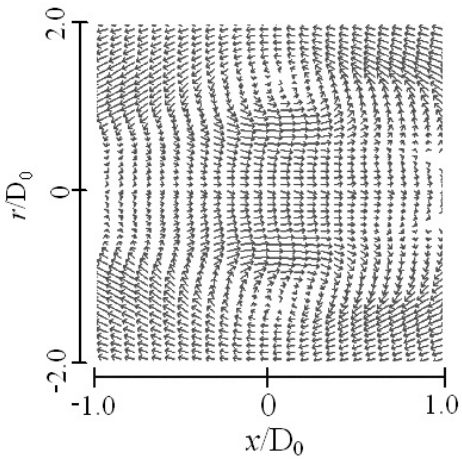

Fig.7 Vortex ring structure for S*=1.0 and Re=1.0x10^4.

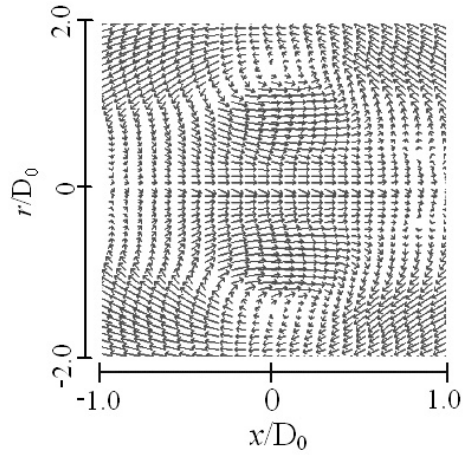

Fig.8 Vortex ring structure for S*=3.0 and Re=1.0x10^4.

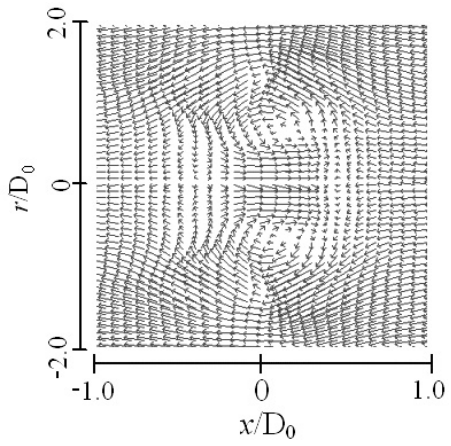

Fig.9 Vortex ring structure for S*=1.0 and Re=4.0x10^4.

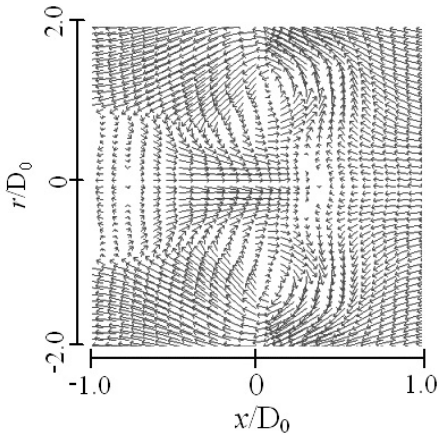

Fig.10 Vortex ring structure for S*=3.0 and Re=4.0x10^4.

Two-dimensional flow field

Fig.6 shows two-dimensional velocity vector field obtained by three transducers. The velocity vector shown in (b) is relative velocity to the translational velocity measured by transducer A so that the circulation structure is easily identified.

Figs.7-10 shows four cases of the two-dimensional flow field in relative velocity. Fig.7 is the result of short stroke and low speed, Fig.8 just longer stroke, Fig.9 just higher speed and Fig.10 longer stroke and higher speed than (a). The result tells us that the increase of piston speed makes the structure of vortex ring clear and its circulation becomes strong while its size hardly changes. On the other hand, as the piston stroke increases, the diameter of the vortex ring becomes large.

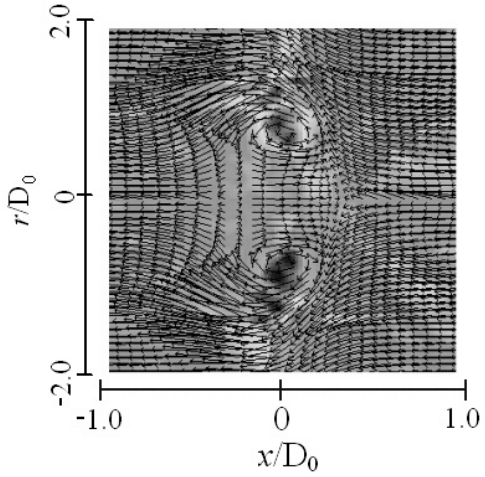

Fig.11 Vorticity distribution in Case 34 (S*=2.2, Re=6.0x10^4)

Fig.11 shows the vorticity distribution in Case 34 (see Table 1). The relative velocity vectors are overlapped on the vorticity color map. We can see that the peak vorticity appears approximately on the point at which the relative velocity vector gets zero. In the case of faster piston velocity given, multiple vorticity peaks emerge but the sign of the vorticity is the same. This implies that the vortex ring with a fast translational velocity would take a relaxation time to be stabilized. It means, the initial structure of the vortex ring, which involves short wavelength disturbance, remains in the present measurement volume. However the measurement error should be evaluated as well, which causes due to several factors including curved motion of vortex ring.

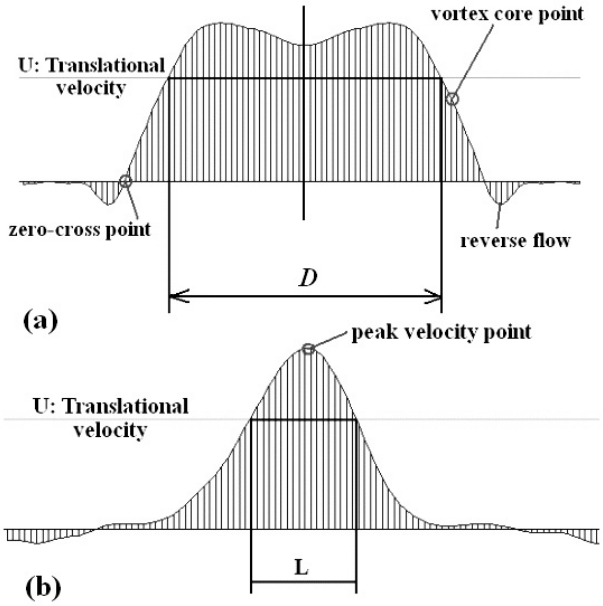

Fig.12 Definition of the diameter and the length of vortex ring

Typical length scales

Using the velocity vector field data of the vortex ring, the diameter and the length of vortex ring have been calculated. The diameter of vortex ring; *D* is defined by the distance between two points, on which the axial component of the relative velocity vector corresponds to zero. Namely, that is the point having the translational velocity. It is not defined with the point of vorticity peak (see Fig.12 (a)). The axial length of vortex ring; *L* is defined by the distance between the two points on the central axis, on which the axial component of the relative velocity gets zero (see Fig.12 (b)).

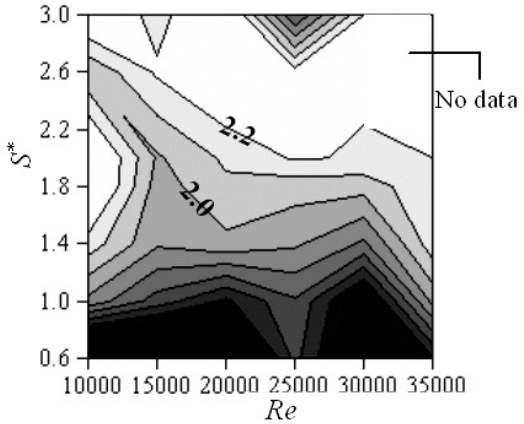

Fig.13 Dimensionless vortex ring diameter

Fig.13 shows the measurement results for the vortex ring diameter normalized by the nozzle diameter D_0, i.e. $D^*=D/D_0$. The grayscale map is drawn as function of dimensionless stroke and Reynolds number in the same way as in Fig.5. It is known that the spatial development of vortex ring is classified into four phases, i.e., generation region, laminar region, wavy region, and turbulent region before breaking up as shown in Fig.14. In the present measurement, the vortex ring from generation region to laminar region is measured. Roughly speaking, the diameter measured at $x=5D_0$ is reduced by increasing the piston speed V or Reynolds number. This is because initial circulation given by the piston gets large with increasing V, resulting in faster generation of vortex ring. However, in the case of V=100mm/s ($Re=1.0\times10^4$), the diameter is exceptionally small because vortex ring itself was not formed clearly. For V>500mm/s ($Re>5.0\times10^4$), the reduction of the diameter becomes blunt. On the other hand, increasing the piston stroke S^* for S* >1 promotes the growth o the diameter. Diameters of more than twice the cylinder diameter were obtained for $S^*>2$.

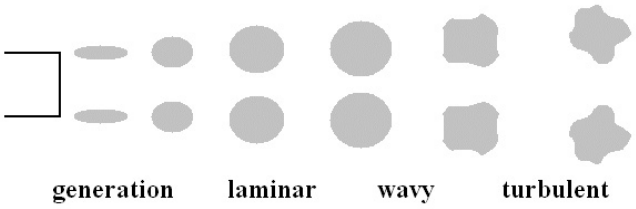

Fig.14 Spatial development of vortex ring in four phases

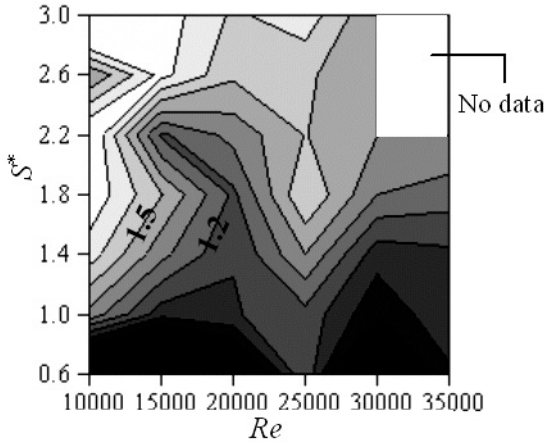

Fig.15 Dimensionless vortex ring length

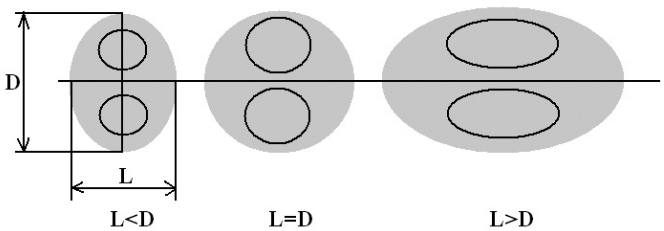

Fig.16 Translating region varied by length of vortex ring

Fig.15 shows the measurement result for the axial length of the vortex ring. The length is one of parameters represent the initial structure of vortex ring produced by piston-type vortex ring generator as shown in Fig.16. In general, the vortex ring length is elongated with increasing the piston stroke S^*. This is because the total volume of translating fluid inside the vortex ring is proportional to the piston stroke. Supposing that any vortex ring is generated ideally and similarly, the vortex ring length must be completely proportional to the piston stoke. However, the actual length of the vortex ring is more complicated for two reasons. One is the fact that the diameter and the length of vortex ring are dependent on each other, and must satisfy the momentum given by the generator. Therefore, the relationship between the diameter and the length is not linear, resulting in non-symmetric structure generated as the piston stroke varies. This tells us simultaneously that there is a suitable relationship between the piston stroke and the piston speed to generate stable vortex ring in the initial region.

CONCLUDING REMARKS

The flow structures of single vortex rings in quiescent water have been successfully measured using UVP. At this time, the vortex ring is generated by a piston-type vortex ring generator, whose behavior varies with two parameters, i.e. the piston stroke D, and the piston speed V. The following points have been confirmed through the present experimental research.

(1) The two-dimensional velocity vector field of vortex ring can be reconstructed by combining three measurement data sets of UVP aligned at different angles. Using the vector maps, the basic characteristics of the vortex ring are quantitatively evaluated using the translational velocity U, the vortex ring diameter R, and the vortex ring length L.

(2) There is a suitable region to generate clear and strong vortex rings on the map of dimensionless piston stroke S^* and dimensionless piston speed denoted by Reynolds number. When the stroke S^* and Re numbers are too small, no clear vortex ring is identified. When the stroke S^* is too long, the flow becomes like a jet which does not induce vortex ring in a short time. When Re number is too large, the vortex ring is unstable and takes a relaxation time to become stable one.

(3) The vortex ring diameter D^* gets large as Re number increases. The diameter is approximately proportional to the piston stroke S* for the range of $1<S^*<3$. The vortex ring length L^* increases with increase of Re number but it is not the monotonic function of Re number.

On the other hand, we encountered the following technical problems in UVP for the application to vortex ring. We have to consider these problems in the next step.

(a) The dynamic range of the velocity measurement by UVP is limited but the core part of the vortex ring had a very high-speed flow obeying the free vortex motion. In case of high piston speed for V>600mm/s, the core part of the vortex ring could not be measured, at which the velocity gets faster than 1m/s.

(b) In the case of slow piston speed or short piston stroke, the hydrogen bubble's buoyancy, which induces no uniform convection of water in the measurement volume, cannot be ignored relative to the main flow.

(c) In some cases, the trajectory of the vortex ring is curved and departs from the measurable radius R.

ACKNOWLEDGMENT

The authors of this paper are grateful for the support by the international academic collaboration program of Hokkaido

University Japan. We also thank to Prof. Greg King, and Mr.Paul Hackett in University of Warwick UK for great help in the experimentation.

REFERENCES

1. Maxworthy, T., 1972, The structure of vortex rings, *J. Fluid Mech*., 51, pp.15-32.
2. Maxworthy, T., 1977, Some experimental studies of vortex rings, *J. Fluid Mech*., 81, pp.465-495.
3. Letchford, C.W., Chay, M.T., 2002, Pressure distributions on a cube in a simulated thunderstorm downburst, *J. Wind Eng. & Industrial Aerodynamics*, 90, pp.733-753.
4. Ishizuka, S., Murakami, T., Hamasaki, T., Koumura, K., Hasegawa, R., 1998, Flame speeds in combustible vortex rings, *Combustion & Flame*, 113, pp.542-553.
5. Renard, P., Thevenin, D., Rolon, J.C., Candel, S., 2000, Dynamics of flame/vortex interactions, *Progress in Energy and Combustion Sci*., 26, pp.225-282.
6. Buchholz, J.H.J, Sigurdson, L.W., 2002, An apparatus to study the vortex ring structure generated by a bursting bubble, *Measurement Sci. & Tech.,* 13, pp.428-437.
7. Tang, S.K., Ko, N.W.M., 2001, Mechanism for sound generation in inviscid two-dimensional vortex interactions, *J. Sound & Vibration*, 21, 823-846.
8. Zhao, F., Lai, M., Harrington, D.L., 1999, Automotive spark-ignited direct-injection gasoline engines, *Progress in Energy & Combustion Sci*., 25, pp.437-562.
9. Fukumoto, Y., 2002, Higher-order asymptotic theory for the velocity field induced by an inviscid vortex ring, *Fluid Dynamics Research*, 30, pp.65-92.
10. Shariff, K., 1992, Vortex rings, *Annu. Rev. Fluid Mech*., 24, 235-279
11. Schram, C., Riethmuller, M.L., 2001, Vortex ring evolution in an impulsively started jet using digital particle image velocimetry and continuous wavelet analysis, *Meas. Sci. Tech*., 12, pp.1413-1421.
12. Willert, C., 1997, Stereoscopic digital particle image velocimetry for application in wind tunnel flows, *Meas. Sci. Tech.,* 8, pp.1465-1479.
13. Takeda, Y., 1995, Instantaneous velocity profile measurement by ultrasonic Doppler method, *JSME Int. J., series B,* Vol.38 (1995) No.1.